



# AgriTera: Accurate Non-Invasive Fruit Ripeness Sensing via Sub-Terahertz Wireless Signals

Sayed Saad Afzal<sup>†</sup>  
MIT  
afzals@mit.edu

Atsutse Kludze<sup>†</sup>  
Princeton University  
kludze@princeton.edu

Subhajit Karmakar  
Princeton University  
sk6051@princeton.edu

Ranveer Chandra  
Microsoft  
ranveer@microsoft.com

Yasaman Ghasempour  
Princeton University  
ghasempour@princeton.edu

## ABSTRACT

The ability to assess the quality of fruit and vegetables at scale can revolutionize the agriculture sector and significantly reduce food waste. In this paper, we present AgriTera, a novel solution for accurate non-invasive, and contract-free fruit ripeness sensing via sub-terahertz wireless signals. The key idea is that sugar and water concentrations in fruit (that are associated with fruit ripening) leave unique non-uniform footprints in the wide band spectrum of the reflected signal off of the fruits. AgriTera utilizes the sub-THz bands for its wide bandwidth, sensitivity to water, mm-scale penetration depth, and non-ionizing features that offer high-resolution inferences from the peel as well as the pulp underneath the peel. We develop a chemometric model that translates the reflection spectra to well-known ripeness metrics, namely Dry Matter and Brix. We conduct extensive over-the-air experiments with commercially available sub-THz transceivers. We compare our results with ground truth values captured by a specialized quality sensor and a vision-based scheme that infers ripeness based on changes in the appearance of the fruit. We demonstrate that AgriTera can accurately estimate Brix and Dry Matter in three different types of fruit with an average Normalized RMSE value of 0.55%, an error that yields a negligible impact on taste and is imperceivable by the consumer.

<sup>†</sup> These authors contributed equally to this work.



This work is licensed under a Creative Commons Attribution International 4.0 License.

ACM MobiCom '23, October 2–6, 2023, Madrid, Spain

© 2023 Copyright held by the owner/author(s).

ACM ISBN 978-1-4503-9990-6/23/10.

<https://doi.org/10.1145/3570361.3613275>

## CCS Concepts

• **Computing methodologies** → **Model verification and validation.**

## Keywords

Sub-Terahertz, Mobile Networking, Food Sensing

## ACM Reference Format:

Sayed Saad Afzal<sup>†</sup>, Atsutse Kludze<sup>†</sup>, Subhajit Karmakar, Ranveer Chandra, and Yasaman Ghasempour. 2023. AgriTera: Accurate Non-Invasive Fruit Ripeness Sensing via Sub-Terahertz Wireless Signals. In *The 29th Annual International Conference on Mobile Computing and Networking (ACM MobiCom '23)*, October 2–6, 2023, Madrid, Spain. ACM, New York, NY, USA, 15 pages. <https://doi.org/10.1145/3570361.3613275>

## 1 INTRODUCTION

Food waste is one of the greatest economic and ethical challenges facing the world today [2, 25]. According to the United Nations, nearly half of the fruits and vegetables produced worldwide are wasted each year [4]. In the United States alone, nearly 30% of all food, worth approximately \$48.3 billion, goes to waste each year [3]. Inefficiency at this scale is only seen in the food industry. A large amount of fruit and vegetables perishes during transport and distribution [42]. Another major reason for waste is that fruits in the market may fail to meet retailers' standards for color and appearance [1, 40]. Today's quality control processes in sorting lines, distribution systems, and retailers are still mostly random and their accuracy is highly limited [14]. Random sampling results in entire batches being rejected, containing both acceptable and damaged fruit and vegetables. On the other hand, performing a close assessment of every fruit would yield significantly higher labor costs and time overhead. Therefore, an automated, non-invasive accurate, and scalable quality sensing mechanism has remained an open problem.

This paper presents AgriTera a novel end-to-end system for non-invasive and scalable fruit quality and ripeness estimation. The process of fruit ripening involves a series of physiological changes and internal chemical reactions. As the fruit ripens

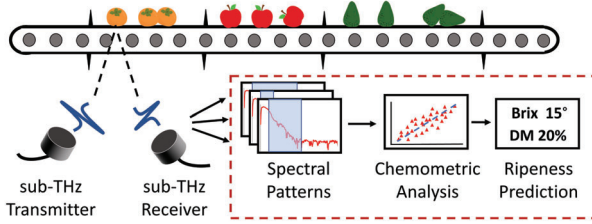


**Figure 1: AgriTera Fruit Ripeness Sensing.** The figure shows the end-to-end system for AgriTera. A broadband receiver measures a sub-THz signal after it reflects off the fruit surface and extracts unique spectral features that correlate well with the fruit’s physiological state. AgriTera uses these features to perform chemometric analysis and estimates the ripeness metrics such as Brix and Dry Matter.

post-harvest, the amount of starch is converted to sugar, leading to changes in the dielectric properties of the fruit. We propose a new technique that aims to extract such internal dielectric variations by investigating the interaction of an impinging sub-terahertz (sub-THz)<sup>1</sup> electromagnetic waves on the fruit. In particular, the internal dielectric properties of fruit leave unique spectral footprints in the spectra of the signals reflected from the fruit. AgriTera is the first system that provides ripeness profile signatures in sub-THz regimes.

These high-frequency bands are a promising candidate for fruit quality sensing: First, thanks to a large amount of bandwidth and their mm/sub-mm scale wavelength, these bands offer higher sensing resolution than microwave and lower millimeter-wave regimes [20]. Second, unlike light and camera-based techniques, sub-THz signals can penetrate through the peel and carry inferences from the internal pulp of the fruit (underneath the peel) [21]. Such inferences are important as the outward appearance of a fruit does not always accurately represent its ripeness, quality, or taste. Third, sub-THz signals show high sensitivity to water and humidity [38]. Since the water concentration in the pulp correlates with the fruit ripening, having a higher sensitivity to water is desired. Finally, sub-THz radiation is non-ionizing and hence it does not damage the fruit under exposure [48].

Fig. 1 illustrates an example deployment scenario. AgriTera can be deployed in multiple stages of the food supply chain. It enables an automated, non-invasive, accurate, and scalable quality sensing mechanism that can be deployed in sorting lines, distribution systems, and retailers. Currently, almost all control quality systems are manual, labor costly, and involve random sampling. AgriTera can be utilized in factories to assess fruit quality before packaging, or in warehouses to

evaluate the fruits’ condition prior to shipment to distributors for sale. Furthermore, it can serve as a valuable tool in retail stores, enabling customers to assess the quality of fruits before making a purchase. AgriTera is a *non-invasive* and non-destructive sensing technique, i.e., it does not involve altering the fruit (e.g., cutting, extracting juice, etc.). Further, AgriTera is a *contact-less* solution as the transmitter and receiver do not need to be in physical contact with the fruits, as shown in Fig. 1. Hence, AgriTera is a scalable solution that can be automated for fruit quality sensing at near zero labor cost and without human involvement.

We first characterize the spectra of the reflected signal by modeling the fruit as a multi-layer dielectric medium. We then analyze the received reflected signal off of the fruit’s body to estimate key ripeness metrics, namely, its solid component without water (called Dry Matter) and the sugar content (called Brix). Changes in Dry Matter and Brix may cause the fruit to be more lossy or transparent to the EM radiations. Hence, we observe that the overall reflected power from the fruit varies over time. However, the total power only provides a coarse-grained estimation of ripeness, as power depends on various other factors (including distance, incident angle, illumination area, etc.).

Instead, AgriTera leverages the relative power variation across a wide band for robust inferences. However, mapping a spectral profile to ripeness metrics come with significant challenges. First, the sensitivity of a particular frequency to ripeness is unknown. More importantly, due to the structural and geometrical diversity in fruits, some frequencies might be more sensitive to the variations in the fruit’s inherent dielectric properties (caused by ripening) than others. In other words, while a particular sub-band in the spectral profile may be a good indicator of the ripeness of one type of fruit, it may contain minimal information for assessing another fruit. To tackle these challenges, AgriTera adopts a Partial Least Squares regression (PLS) model that finds spectral patterns that correlate best with ground-truth Brix and Dry Matter measurements. For each fruit type, AgriTera develops a correlation transform function that estimates Brix and Dry matter from the reflection spectra. We emphasize that AgriTera is a non-coherent sensing method as it only takes into account the power variation, albeit across a wide range of frequencies (and not phase information).

We implement AgriTera using a commercially available ultra-wideband transmitter and receiver. We perform extensive measurements by collecting the reflection spectra of 3 types of fruits at fine-grained time resolution (every 12 hours). We also measure the ground truth values of Dry Matter and Brix using an off-the-shelf specialized sensor that works based on near-infrared spectroscopy and requires physical contact with the fruit (thereby not scalable). As a baseline scheme, we also deploy high-resolution cameras and perform image

<sup>1</sup>We use the term sub-THz to refer to a wideband signal that ranges from 50 to 600 GHz.

processing with the goal of inferring ripeness through changes in the outer appearance of the fruits. Our findings indicate that AgriTera is superior to image-based measurements in detecting physiological changes within the fruit, achieving both high sensitivity and accuracy. This accuracy is also influenced by the bandwidth, allowing for the detection of changes even in over-ripe fruit, which is not possible with Brix and Dry Matter measurements as they reach a plateau.

## 2 PRIMER

In this section, we discuss common metrics used in the food industry to quantify the ripeness of fruits. Furthermore, we explain the insufficiency of the state-of-the-art in enabling accurate and non-destructive fruit ripeness measurements and the potential of sub-THz bands to achieve this goal.

### 2.1 Cycle of Fruit Ripening

Fruits can be classified into two main categories based on the regulatory mechanisms governing their ripening process: climacteric and non-climacteric. Climacteric fruits like kiwi, avocado, apple, and banana will keep on ripening after they have been plucked from the plant [37, 44]. On the other hand, non-climacteric fruits like grapes, oranges, and pineapples halt the ripening process as soon as they are harvested. In this work, we will focus on climacteric fruits (e.g. apples, avocados, persimmons, etc.). These fruits are transported over great distances, both domestically and internationally, in order to serve a wide consumer base and they normally undergo three different maturity stages: (i) Physiological maturity stage, where the fruit can be harvested and will continue to ripen, (ii) Horticultural maturity, where it is ready to be consumed, and; (iii) Overmature stage, where it starts to rot. As a result, it is crucial to harvest and transport the fruits when they reach maturity in order to maximize the time available for transportation and storage, thus enhancing profitability. In addition, the amount of nutrition in fruit is maximum during the horticultural maturity [56]; thereby, it is important from the customer's perspective to know the maturity level of fruit and vegetables.

Determining fruit maturity is, however, not simple, and food scientists employ several factors to determine the quality of produce. Past research has demonstrated that these factors (e.g., dry matter, Brix, titratable acidity, and surface color, etc) are highly correlated with fruit ripeness and can also be used to determine different maturity stages in fruits [12, 30, 39, 43]. Next, we explain each of them in detail.

### 2.2 Ripeness Metrics

**Dry Matter:** As the name implies, the dry matter (DM) of a fruit refers to its solid component without water. Dry matter accounts for various components including sugars, carbohydrates, oils, proteins, starches, antioxidants, vitamins, fiber, lipids, minerals, volatile compounds, and structural

carbohydrates like fiber and skin. The build-up of dry matter in fruit undergoes different changes as it develops, making it an effective measure of maturity in both climacteric and non-climacteric fruits. In principle, when a fruit reaches maturity, it has reached its maximum size and amount of accumulation solids or dry matter.

**Brix or Total Soluble Solids (TSS):** Brix ( $Bx$ ) is taken as a measure of sugar or sweetness of fruits or fruit juices. Brix quantifies the amount of total soluble solids (TSS) present in fruit ( $1^\circ Bx$  refers to 1 gram of sucrose in 100 grams of aqueous solution). TSS is primarily composed of sugars (including monosaccharides, disaccharides, and oligosaccharides, such as sucrose, fructose, etc.), but it also includes other compounds such as minerals, soluble fat, alcohol, and flavonoids (Vitamin C and Vitamin A). Brix is a reasonable indicator of fruit ripeness because it demonstrates the amount of starch is converted to sugar as the fruit ripens post-harvest.

**Fruit Surface Color:** The process of fruit ripening is a well-coordinated and irreversible process that involves several physiological and organoleptic alterations. Certain fruits such as bananas and apples change colors throughout the ripening process, and the most vivid colors generally occur at the ideal ripening point. Green fruits are often unripe and have chlorophyll in their cells, which gives them their green color. As they mature, the chlorophyll deteriorates and gets replaced by the orange pigment carotenoids and the red pigment anthocyanins. These substances are antioxidants that help to protect the fruit from spoiling too soon when exposed to air. Although the color of fruits can sometimes indicate ripeness, it is not reliable or accurate for all fruits as some retain their chlorophyll content even when they are mature, e.g., green apples, pears, limes, etc. Further, color is just a coarse measure of ripeness.

### 2.3 Insufficiency of Existing Solutions

Tracking the maturity of fruit offers advantages for various stakeholders, including farmers, distributors, retailers, and consumers. Nevertheless, the current methods are either destructive, inaccurate, or non-scalable (limited to lab). Some solutions rely on precise chemical measurements (e.g., gas chromatography, mass spectroscopy, ethylene sensing with carbon nanotubes) by analyzing the fruit juice to assess the nutrient content and quality [15, 27, 45]. Even though these measurements offer fine-grained information about the fruit, the fruit is destroyed in the process, and further contributes to the food waste. Other non-invasive chemical techniques utilize the emission of ethylene gas as an indicator of fruit ripeness, but they require fruits to be placed in enclosed containers to keep the gas from escaping, thus limiting their practicality [7, 15]

Given the aforementioned shortcomings of direct measurement, recent advancements looked at camera-based techniques that utilize computer vision algorithms to identify defects or



color changes in fruit images. These methods typically rely on machine learning algorithms to extract features from visual cues [60]. However, most fruit ripen and rotten from the inside and changes in color often occur very gradually or not at all for many types of fruit.

The goal to develop a non-destructive, high-resolution, and reliable fruit sensing technology has recently prompted researchers to utilize chip-based sensors equipped with LC resonators that can be attached directly to fruits and vegetables [58]. However, these approaches necessitate a specialized sensor for each type of fruit that are sensitive to specific chemical indicators of fruit spoilage. Additionally, these tags should be in direct contact with the fruit, yielding possible contamination and significant labor costs for attaching these tags to each individual fruit.

Unlike previous literature, this paper presents an accurate, non-destructive, and contactless wireless sensing for fruit ripeness. Specifically, we leverage sub-terahertz (50-600 GHz) signals to *see beneath* the peel of fruits and infer the ripeness metrics through their footprint on the spectral properties of reflected sub-THz signals.

## 2.4 Why Sub-Terahertz bands?

More recently, multiple works have demonstrated the potential of wireless signals to monitor and assess fruit quality, albeit at different frequencies [24, 35, 41]. Yet, sub-THz bands have unique features that make them a promising candidate for wireless fruit ripeness sensing. Specifically, the large bandwidth, mm-scale penetration depth, and high sensitivity to water make sub-THz signals an attractive modality for high-resolution wireless ripeness sensing.

**WiFi and mmWave:** Previous research has demonstrated that it is possible to extract features from the WiFi (2.4 GHz - 5 GHz) and mmWave (60 GHz) bands. Fruit quality assessment in WiFi is typically achieved by taking advantage of the large penetration depth offered at these low frequencies. From this, the estimated changes in the refractive index of the fruit and the physiological changes occurring within it (obtained by WiFi packets transmitted through the fruit for channel state information (CSI) extraction), are correlated to fruit ripeness. Other methods either examine the fruit from multiple sides [50, 59] or use tags [47]. However, given the low bandwidth, and henceforth resolution, techniques that use WiFi can only provide a qualitative assessment of ripeness (e.g. unripe, half-ripe, ripe, overripe, etc) [35, 59]. Wireless signals in the mmWave band (60 GHz) have been applied in the domain of fruit sensing to determine the Brix value of different fruits [61]. The key technique relies on obtaining the reflected signal's RSSI after it travels through the fruit. However, as mmWave signals are relatively narrow-band, containing only a few gigahertz, the information in their spectrum is insufficient to allow for precise assessment of fruit quality.

**Near Infrared (NIR) Spectroscopy:** Various types of commercial sensors can sense the quality of crops using NIR spectroscopy [9]. To evaluate the quality of the fruit, an NIR pulse is transmitted to the sample's surface and the resulting reflection is measured. Typically, laboratories use benchtop NIR sensors that are pre-calibrated for specific commodities (fruits, vegetables, dairy, etc.) or certain analytes (carbohydrates, sugars, fats, etc) within those commodities. Another class of sensors is referred to as "Inline sensors". These work together with the sorting line in warehouses to gather information about the dry matter or color of the fruits that are moving along the conveyor belt. Although these can provide data at relatively high throughput, they are incapable of generating high-resolution data and are limited to providing only coarse information about fruit quality metrics [33]. The third group of NIR sensors are portable yet expensive devices that offer detailed information regarding the quality of the fruit [11]. However, since signals in the NIR spectrum have limited penetration capability, the sensor must come into direct contact with the fruit to collect reliable data, hindering the scalability of such solutions.

**Advantages of Sub-THz Bands in Fruit Sensing:** Similar to WiFi and mmWave bands, sub-THz signals can penetrate through the body of fruit and see beneath the peel; yet, unlike those bands, sub-THz signals can carry much richer information given their larger bandwidth. While the accuracy of sub-THz measurements is comparable with near-infrared, sub-THz signals experience less propagation loss and hence can operate without being directly in contact with the fruit. Moreover, the sub-THz band encompasses frequencies that resonate with water molecules, making it an excellent candidate to measure moisture levels in fruits, which significantly influence their Brix and Dry matter content.

## 3 AgriTera

In this section, we explain the key components of AgriTera for accurate non-invasive fruit quality sensing.

### 3.1 System Overview

AgriTera is a novel system that non-intrusively determines the quality of fruit by identifying and measuring the ripeness-sensitive signatures in the sub-THz reflection profile off of fruits. Our key insight is that the chemical reactions inside the fruit associated with the ripening (including the moisture concentration) impact the reflection properties of sub-THz signals that penetrate into the fruit pulp, providing inferences from under the peel. The fruit ripening process involves a series of changes in the composition of the fruit, that is triggered by a cascade of chemical and biochemical reactions in the fruit (including changes in water concentration). As a result of the changes in the fruit's chemical composition, its electromagnetic properties would vary over time, yielding

changes to the interaction of the sub-THz wave with the fruit body and pulp. Building on top of these insights, we then devise a model that characterizes the correlation between the spectral profile of reflected signals off of fruit and their inherent time-varying EM properties. Exploiting our model, we then correlate ripeness-specific spectral signatures in the reflection profile with well-known ripeness metrics such as Dry Matter and Brix, providing a framework to predict the quality of fruit by solely relying on the spectral profile of sub-THz signals as they interact with the fruit.

### 3.2 Footprint of Fruit Quality on the Reflected sub-THz Signals

In this section, we characterize the reflected signal off of the fruit as a function of its physiology. To this end, we model fruits as a multi-layer medium with certain permeability and permittivity profile. Permittivity ( $\epsilon$ ) is a measure of the electric polarizability of a dielectric, i.e., how easily it polarises in response to an electric field. Further, permeability ( $\mu$ ) is the measure of magnetization that a material obtains in response to an applied magnetic field. Permittivity and permeability are inherent properties in a material that captures its interaction with electromagnetic waves. These two parameters define the refractive index of a medium, which determines how much electromagnetic waves are bent, or refracted when entering a material. In general, the refractive index is a frequency-dependent dimensionless number that can be written as  $n = \sqrt{\epsilon_r \mu_r}$ , where  $\epsilon_r$  is the material's relative permittivity, and  $\mu_r$  is its relative permeability. Most naturally occurring materials are non-magnetic at sub-THz frequencies, that is  $\mu_r$  is very close to 1 [6], therefore  $n$  is approximately  $\sqrt{\epsilon_r}$ . Under this approximation, the complex refractive index  $n$  follows the relation:

$$n(f) = \sqrt{\epsilon_r} = n_r(f) + jn_i(f) \quad (1)$$

The real part of the refractive index,  $n_r$ , is responsible for the bending or scattering of the electromagnetic wave as it enters another medium. The imaginary part,  $n_i$ , is known as the “extinction coefficient”, and is a measure of the electromagnetic wave absorption in the medium. Both the real and imaginary parts of the refractive index are frequency-dependent, which means they vary across the spectrum.

Fig. 2 depicts our multi-layer fruit model. Fruits consist of three primary layers, namely the exocarp, which forms the hard outer skin, the mesocarp, which constitutes the bulk of the fleshy fruit, and the endocarp, the innermost layer that encases the seed. Each of these layers has a distinct refractive index, which we denote as  $n_1$ ,  $n_2$ , and  $n_3$  respectively. The process of fruit ripening involves a series of physiological changes that contribute to changes in the permittivity of the internal layer of fruit. Therefore, the refractive index of a fruit can be used as an indicator of its internal quality.

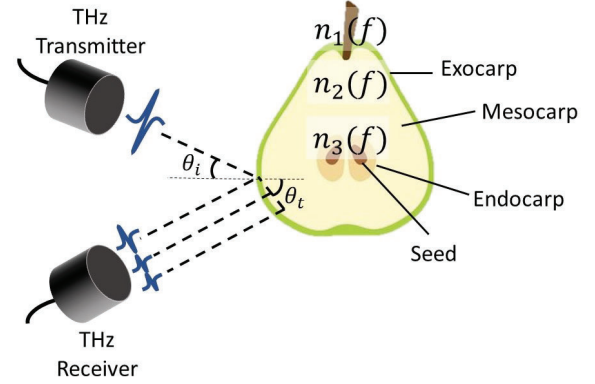


**Figure 2: Fruit as a multi-layer dielectric medium.** We model fruit as a multi-layer structure such that each layer has a different permittivity and permeability and hence a different frequency-dependent refractive index ( $n$ ). As a result, different frequencies are reflected and absorbed by these layers resulting in a unique pattern in the reflection spectra.

AgriTera relies on the spectral signatures in the reflected signal from all layers of the fruit for ripeness sensing. As the signal penetrates through the different layers, the electric field decays due to absorption. Hence, in practice, the penetration depth of 0.3mm is expected for frequencies between 100-400 GHz [62]. Therefore, the reflection profile contains inferences from the peel (i.e., exocarp) and pulp (i.e., mesocarp) of the fruit combined, as shown in Fig. 2. This combined reflected power  $P_r$  can be characterized as following<sup>2</sup>:

$$P_r(\theta_i, f) = \sum_k P_{ik} R_k(\theta_i, f) \quad (2)$$

$$R_k(\theta_i, f) = \left( \frac{n(f)_{k-1} \cos(\theta_i) - n(f)_k \cos(\theta_t)}{n(f)_{k-1} \cos(\theta_i) + n(f)_k \cos(\theta_t)} \right)^2$$

where  $k$ ,  $f$ ,  $\theta_i$ , and  $\theta_t$ , represent the index of each layer, frequency, angle of incidence, and angle of refraction (after bending) respectively while  $P_{ik}$ ,  $R_k$ , and  $n(f)_k$ , denotes incident power of the sub-THz signal, the reflectance, and the refractive index at each layer with index  $k$ .  $\theta_t$  is also known as the angle of refraction and can be written as a function of  $\theta_i$  using Snell's law (i.e.,  $n(f)_{k-1} \sin(\theta_i) = n(f)_k \sin(\theta_t)$ ). Although the total reflected power is correlated to changes in the complex refractive index of the fruit, it is not a robust measure of fruit quality on its own since it also depends on the fruit distance to the TX/RX, the scattering properties of the fruit surface, the illumination area on the fruit, and the impinging angle. Instead, AgriTera relies on the relative

<sup>2</sup>Assuming perpendicular polarization. Extension to parallel polarization is straightforward.

spectral signature across a range of frequencies to infer the fruit's physiology.

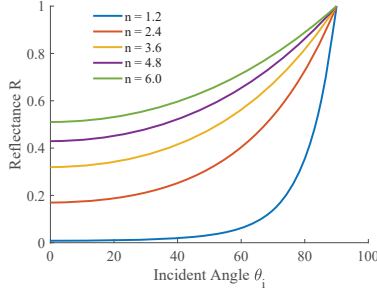


**Figure 3: Incident Angle vs Reflectance.** The amount of reflected power or reflectance is a function of incident angle. Reflectance increases with larger incident angles.

### 3.3 Valid Range of Incident Angles

As seen in Eq. (2), the angle of incidence plays a key role in the amount of reflected power. To determine the optimal range of incident angles for AgriTera we plot the reflectance as a function of the incident angle  $\theta_i$  for single-layer fruit in Fig. 3. For simplicity, we consider a frequency-independent refractive index in the range of 1.2 to 6, as reported in the prior work [29]. The first key observation is that regardless of the fruit's refractive index, total reflection is always achieved at  $90^\circ$ . However, using  $90^\circ$  as the incident angle is not practical because it would require a significant distance between the transmitter and receiver. The second observation is that higher incident angles lead to a better SNR because the reflected signal is stronger. However, this only applies to reflections from the surface of the fruit. Since we're interested in reflections from *beneath* the peel, we can't solely rely on this result to determine the optimal angle.

When the signal is incident close to the surface normal (i.e.  $\theta_i = 0$ ), the reflection is weakest, and the penetration depth (which measures how deep electromagnetic radiation can penetrate into a material) is maximized. To confirm this, we used a COMSOL simulation to analyze a 150 GHz signal impinging on a fruit surface at different incident angles (shown in Fig. 4). The fruit body was modeled as a single-layer structure with a refractive index comparable to actual fruits to demonstrate the penetration inside a fruit. As shown, smaller incident angles result in lower reflected power, but also larger penetration (as more of the signal refracts), allowing us to capture more interactions with the pulp. On the other hand, larger incident angles result in higher reflection power on the surface, but a weaker reflected signal from the pulp. Based on this, the optimal position for AgriTera is at an incidence angle of 45 degrees, which is in the middle of the overall incident angle range.

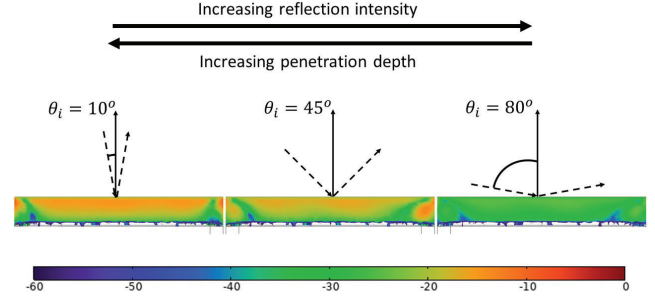


**Figure 4: EM Simulation Results of Sub-THz Penetration.**

The figure shows the normalized penetration intensity pattern heat (in dB) inside a fruit sample when a 150 GHz signal is impinging on the surface at three different incident angles. The red color represents higher intensity while blue shows weaker signal strength. The penetration of the signal through the fruit reduces with increasing incident angle.

### 3.4 Chemometric Analysis for Ripeness Prediction and Inference

Thus far, we have modeled the spectral profile of the reflected sub-THz signal as a function of the fruit refractive index that varies over time due to internal chemical reactions related to fruit physiology. However, to have a reliable estimation of fruit quality, it is critical to estimate the key metrics such as Brix and Dry Matter from such measured spectral profile (see §2.2). Hence, our goal is to introduce a systematic framework to accurately map the spectral signatures in the sub-THz regime to the Brix and Dry Matter parameters, as shown in Fig. 5.

The mapping of the spectral signatures to a scalar value (such as Brix and Dry Matter) is not straightforward: First, obtaining accurate measurements of Brix or Dry Matter by merely analyzing statistical properties of the reflected spectrum (such as mean or max amplitude) is not feasible as these features depend on various other factors (including distance, incident angle, illumination area, etc.). Second, the captured power is correlated across the spectrum, albeit, through an unknown and non-linear function that may also differ with various fruit types, so extracting data that is sensitive to ripeness metrics from a correlated spectrum is challenging. Further, it's hard to decide the frequency band of operation since the contribution of certain frequency sub-bands to Brix or Dry Matter levels might be minimal while other sub-bands observe a strong correlation with Brix, Dry Matter, or both.

To tackle these challenges, AgriTera adopts a Partial Least Squares regression (PLS) model to extract ripeness metrics from the sub-THz spectrum. We opted for PLS because it provides two benefits for our ripeness-sensing application. First, it produces a model that maximizes the correlation



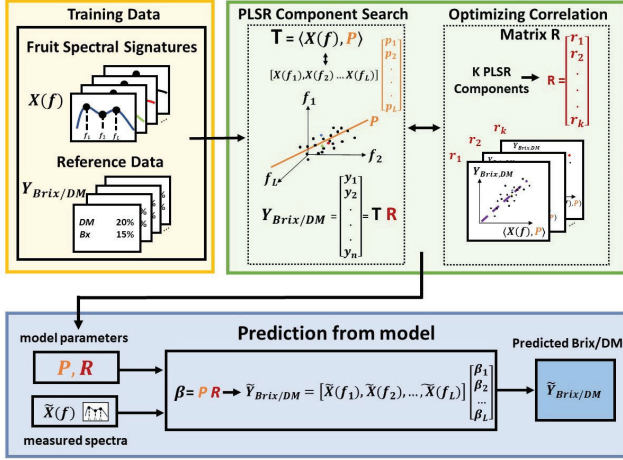


**Figure 5: Chemometric Analysis.** The figure shows our two-step chemometric analysis. In the training step, AgriTera searches for the PLSR components that are highly correlated with the ripeness metrics and find their corresponding scores. In the prediction step, those weighted components are used to map the measured spectra to Brix and Dry Matter values.

between the ripeness metrics and the spectra. Second, it enables us to represent the entire spectrum data using fewer components, resulting in a lower-rank representation that focuses solely on relevant information in the spectrum.

To generate a model, PLS specifically utilizes the sub-THz spectrum (variable data) acquired from the signal reflected off the fruit body, as well as the ground truth Brix and Dry Matter values. PLS then performs PCA on the variable data  $X(f)$  and correlates it with measurement values  $Y_{Brix/DM}$  in order to establish a mapping between the spectrum and the measured values for ripeness metrics. This gives PLS the following representation for  $X(f)$ :

$$X(f) = TP' + E, \quad (3)$$

where  $X(f)$  is an  $N \times L$  matrix with  $N$  sub-THz measurements and  $L$  frequencies,  $T$  is a matrix that holds the scores or projections on the PLSR components with a matrix size of  $N \times K$  where  $K$  indicates the number of PLSR components ( $K < L$ ). Finally,  $P'$  is a matrix (with size  $K \times L$ ) that contains the contribution of each PLSR component for a particular frequency in  $X(f)$ .  $E$  is a matrix that stores the unexplained information, i.e., the residuals.

Although it may seem like PLS is simply performing PCA on the spectrum data, it is actually more complex than that. While PCA identifies the major variations in  $X(f)$ , PLS searches for a direction of the principal component that is useful for correlating scores ( $T$ ) with measured values in  $Y_{Brix/DM}$  (with size  $N \times 1$ ) in the training phase. In other words, PLS looks for relevant information in  $X(f)$  that is highly

correlated with Brix or Dry Matter readings. In particular, we establish a correlation vector  $R$  ( $K \times 1$ ) between  $T$  (scores of  $X(f)$ ) and  $Y_{Brix/DM}$ . From this, we define a coefficient matrix  $\beta = PR$  that maps the measured power spectrum to an estimated Brix and Dry Matter value in the testing phase as follows

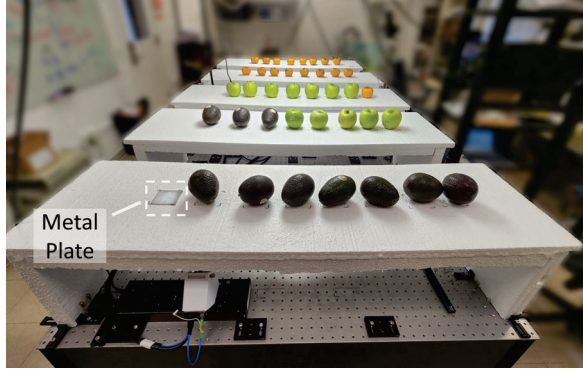
$$\begin{aligned} Y_{Brix/DM} &= TR \\ \beta &= PR \\ \tilde{Y}_{Brix/DM} &= \tilde{X}(f)\beta \end{aligned} \quad (4)$$

One key advantage of using PLS for this application is that it can withstand minor variations in the measurements of brix and dry matter content in fruit. This is important because the sensor's placement on the fruit can cause slight fluctuations in the measured readings  $Y_{Brix/DM}$  which can impact the training phase. By being robust to such fluctuations, PLS can produce an accurate model that captures the key indicators of fruit ripeness.

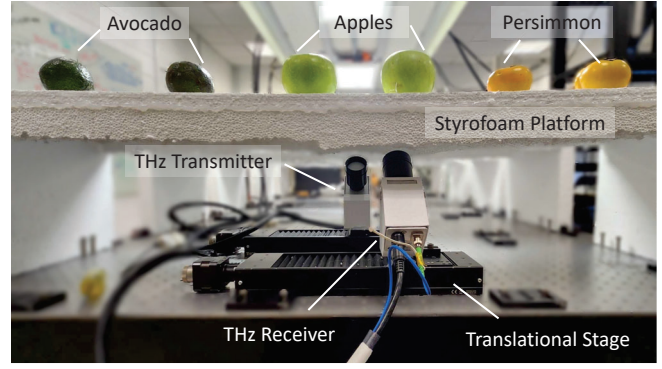
## 4 IMPLEMENTATION & EXPERIMENTAL SETUP

We evaluate the performance of AgriTera through extensive over-the-air experiments. Fig. 6 illustrates our overall experimental setup. We create a conveyor belt-like setting by positioning the fruits on a styrofoam platform. The transmitter and receiver are placed underneath the platform as shown in the figure. Styrofoam has low absorption in the sub-THz range [63]; hence, it allows the emitted energy to pass through the platform and impinge on the fruit with negligible loss. Other plastic surfaces such as HDPE can also be used as alternatives.

For transmission and reception, we use a time-domain broadband system (TeraMetrix T-Ray [36]) that produces an ultra-short pulse with a bandwidth of 5 THz but a flat frequency response between 100 GHz to 400 GHz. We use bandpass filters to isolate the band of interest. The detector measures the electric field magnitude at a wide range of frequencies with a spectral resolution of 1.22 GHz. The emitter and detectors are both linearly polarized with a polarization extinction ratio of 20:1. We collect raw time-domain samples and apply conventional signal processing techniques (smoothing, filtering, FFT, etc.). Note that even though our testbed provides time-domain waveforms, AgriTera only uses power measurements (albeit across multiple frequencies) for ripeness inferences. This is because phase information at this regime is highly sensitive to the dynamics of the environment, and even the small perturbations on the surface of some fruits (e.g., avocado) can yield randomness in phase. In a typical conveyor belt, the products move on the belt. However, it is hard to realize that in the lab. Instead, we mount the TX/RX

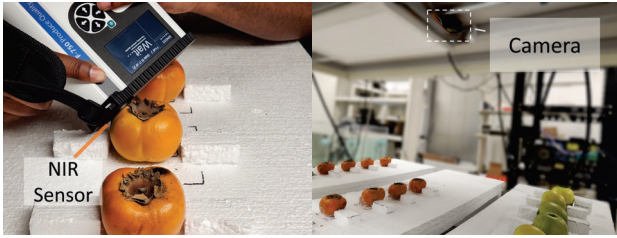


(a)



(b)

**Figure 6: Our Experimental Platform.** The figure shows the overall experimental setup for AgriTera. (a) The fruits are placed on top of a styrofoam platform that is transparent to sub-THz radiations. (b) The sub-THz transmitter and receiver are placed directly below the platform and are mounted on a stage that can be moved to scan all fruits.



(a) Felix Instruments

(b) Camera

**Figure 7: Baseline Fruit Ripeness Devices.**

on a mobile transnational stage and move them (with a controller) to collect data from different fruits. AgriTera utilizes a pre-trained PLSR model tailored to specific fruit types. Each new inference involves a single Fast Fourier Transform (FFT) operation and matrix multiplication. Hence, the process involves low complexity computations ( $O(n \log_2 n)$ ), enabling real-time ripeness inference on a conveyor belt and separation of the fruits based on their maturity.

Recall from section §3.2 there is a tradeoff in the choice of the incidence angle: a larger incident angle (relative to normal) offers higher reflected power (and hence, better signal-to-noise ratio) but the penetration depth is smaller. To balance this trade-off, we mount the TX and RX such that the incident angle on the fruit is about 45 degrees.

We evaluated AgriTera using a total of 30 fruits, namely green apples, avocados, and persimmons. These fruits are chosen because they have different structures, surface properties, peel thickness, and pulp types; hence, they can represent the existing variety of fruits. Nevertheless, AgriTera can in principle provide ripeness inferences for all types of fruits. The number of samples was chosen based on space limitations (size of the conveyor belt emulator). Increasing the sample size

will only improve the accuracy. Investigating the performance of AgriTera for other types of fruits and vegetables will be explored in the future.

We took measurements every 12 hours over the course of 10 days, resulting in a total of 200 measurements for each fruit category. To have a fair comparison across time, the fruits were not moved on the platform during data collection, however, AgriTera is not dependent on fruit shape or orientation. We have conducted measurements on multiple fruits placed in random orientations and our results show that the ripeness estimation is consistent.

**One-time calibration.** Despite the fact that the transmitted pulse is a signal with a wide range of frequencies, the power transmitted is not evenly distributed across all frequencies. Therefore, it is crucial to normalize the received waveform using a reference signal, ideally from a perfect reflector. Additionally, even though the styrofoam platform is almost transparent to the sub-THz signals, it still produces a weak reflection that can alter the spectral profile of the signal. To address these issues, AgriTera performs a one-time calibration by sending a signal to a metal plate situated on the platform (as shown in Fig. 6a) and recording the resulting reflection. This reference signal is then used in data pre-processing to remove any non-linearity by normalizing each measurement with the reference waveform. In addition, AgriTera transmits a signal to the styrofoam (without the fruit) to record the background signal for interference cancellation. It is important to note that this calibration is a one-time procedure as the interference from the styrofoam and the non-linearity of the emitter spectrum is fixed.

**Specialized Brix/Dry Matter Measurement Device.** We use commercial and specialized tools for obtaining the ground truth Brix and Dry Matter values. In particular, we exploit the Felix Instruments F750 Food Quality Sensor [16], which



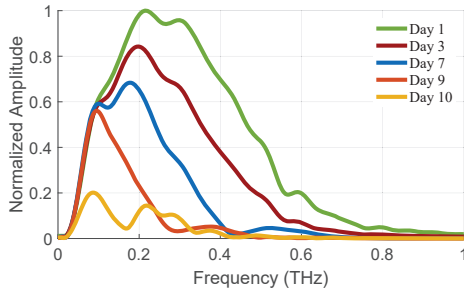


**Figure 8: Sub-THz spectrum for persimmon ripening.** The figure shows how the spectrum changes over time and as the persimmons ripen.

provides Brix and Dry Matter readings for a limited number of fruits. This device works based on near-infrared spectroscopy and costs more than \$10K. This sensor should be put in direct contact with the fruit as shown in Fig. 7a and hence it is not a practical solution to estimate fruit quality at scale. In our experiments, we measure the Brix and Dry Matter of each fruit from multiple angles every 12 hours and compare these values with the prediction results of our chemometric analysis algorithm.

**Image processing as a baseline scheme.** For comparison purposes, we also deploy cameras to capture photos of the fruits at various stages of ripeness, as shown in Fig. 7b. In this baseline scheme, we implement traditional image processing techniques to capture the color change at fine-grained resolution and use it to infer the internal ripeness. In Sec. 5, we compare our results against this baseline scheme.

## 5 EVALUATION

Here, we present the performance of AgriTera with extensive over-the-air experiments.

### 5.1 Initial Feasibility Experiment

AgriTera is built on the idea that the inherent chemical interaction in the fruit pulp would leave a non-negligible footprint in the spectral profile of sub-THz signals interacting with the fruit. As the first step, we validate this hypothesis with a feasibility test. To this end, we directly impinge a wideband pulse on 10 persimmons and measure the reflected signal off of them. We repeat this experiment for 10 days.

Fig. 8 illustrates the spectral profile of the reflected signal over the course of 10 days. We have the following observations: First, the amount of reflected power decays over time; this is likely due to the fact that the persimmon loses moisture and becomes more transparent to the sub-THz signal, resulting in less energy being reflected back. Second, we observe a non-uniform decrease in the amount of reflected power suggesting a frequency-selective signature. Third, such spectral variations happen in wide range of frequencies (50 to 600 GHz),

suggesting frequency-dependent sensitivity to the chemical interactions attributed to fruit ripening and over-ripening (i.e., change in the water and sugar concentration). Our experiments reveal unique spectral sensitivity for each fruit type, indicating the potential for sub-THz frequencies in quality sensing.

### 5.2 Variations of Dry Matter and Brix

In order to gain insight into how Brix and Dry Matter values vary across different types of fruits, we conducted an experiment to monitor these values over a 10-day period. Fig. 10 displays the changes in Brix and Dry Matter levels over time for Persimmons, Green Apples, and Avocados. The data were collected using the Felix Instruments device, which was only capable of providing Brix readings for Persimmons, Dry Matter measurements for Avocados, and both Brix and Dry Matter readings for Green Apples. The plotted values correspond to the median of the values obtained from ten fruits of the same type. The following observations can be made: first, Fig. 10 (a),(b) indicates a general upward trend in Brix values over time, which is expected as starch in the fruit is converted to sugar. We can see that Brix is higher for persimmon compared to green apple which matches the sweeter taste of persimmon. After the fruit ripens, the Brix values reach a plateau. This happens after approximately 120 hours (5 days) for green apples and after approximately 220 hours (9 days) for persimmons. The Brix and Dry Matter measurements show a positive correlation in green apples.

Avocados do not have much sugar content and hence Brix is not defined for them. Instead, in Fig. 10 (c), we see a clear trend in Dry Matter reaching a peak after roughly 100 hours (4 days), i.e., when they become fully ripe. After that, we observe a decline in Dry Matter values (overripe stage).

From Fig. 10, it may appear that the time elapsed after harvest serves as a potential indicator of fruit ripeness. However, it is important to realize that while time after harvest plays a role, it is not the sole determining factor that impacts fruit quality. Other factors, such as humidity, temperature, and proximity to ethylene-emitting fruits, also play significant roles in the ripening process. Therefore, to gain a comprehensive understanding of fruit quality, direct or indirect measurement of Brix and Dry Matter is crucial.

### 5.3 Fruit-Specific Spectral Signatures

As shown in the feasibility experiment, fruit ripening yields non-uniform spectral variations in the reflection spectra. Hence a follow-up question is: which frequency bands display the most correlation with ripening features and consequently provide greater insights into fruit quality?

To answer this question, we leverage our PLSR model. In particular, we look into the contribution of each frequency in the PLSR model for predictions, i.e., matrix  $\beta$  as elaborated in section §3.4. Once the spectra from various fruits are input into the PLSR model, AgriTera utilizes the data to train the



**Figure 9:** The images captured from persimmon over a 10-day period. The images show negligible changes in the physiology of the fruit's skin, making visual detection inaccurate and unreliable.

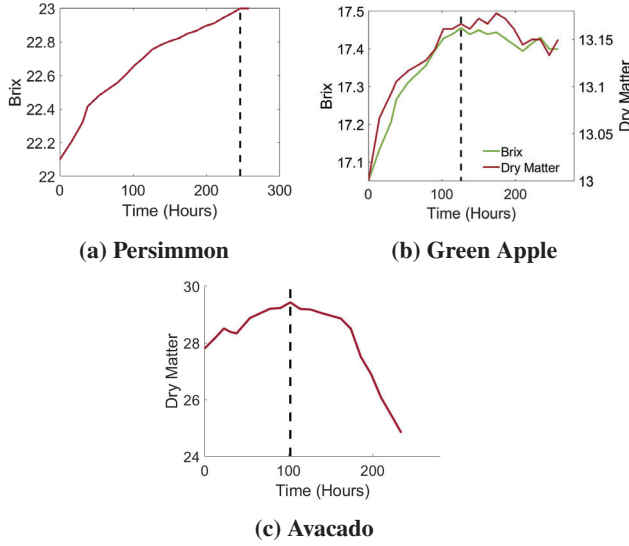


**Figure 10: Measured Trends in Brix and Dry Matter.** The figure plots the Dry Matter and Brix as a function of time for three different fruits. The dashed lines represent when the fruit has reached horticulture maturity.

model and generate the matrices  $P$  and  $R$ , which constitute the PLSR coefficients for predictions, as elaborated in §3.4.

Before training the model, a set of around 20 samples is extracted from the set of approximately 200 samples, which is then reserved to assess the model's performance. This collection of 20 samples includes the measured spectra over 10 days (every 12 hours) for one individual fruit.<sup>3</sup> We do this to evaluate whether the set of ripeness-sensitive frequencies (frequencies that hold the most pertinent information) is consistent for different fruits of the same type. Therefore, we generate 10 total models (10 different  $\beta$  vectors) that can map received spectra to Brix/Dry Matter values.

Fig. 11 illustrates how the normalized PLSR coefficients ( $\beta$ ) change with frequency for various fruits. The plot displays the median (in black), the 75<sup>th</sup> percentile (in blue), and the 25<sup>th</sup>

<sup>3</sup>We initially collected measurements at 1-hour and 8-hour intervals but we did not observe any significant changes in the Brix/Dry Matter values so we opted for 12-hour intervals.

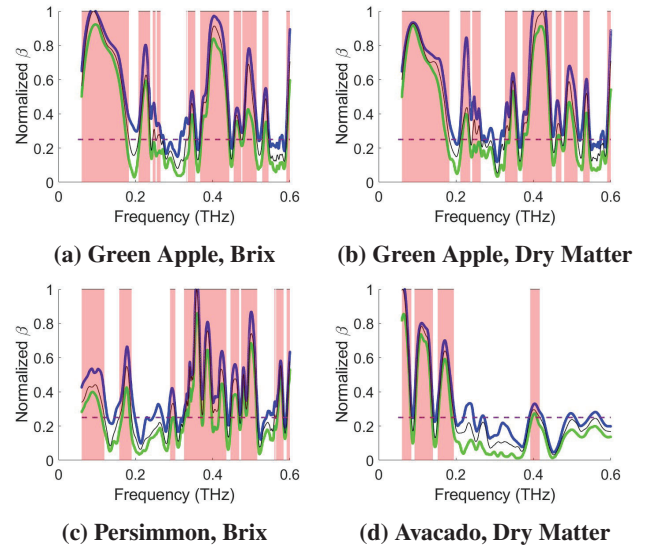


**Figure 11: Fruit-Specific Spectral Footprint.** The figure plots the median normalized PLSR coefficients ( $\beta$ ) in black and the 75<sup>th</sup> and 25<sup>th</sup> percentile in blue and green respectively. The highlighted bands are highly correlated with ripeness metrics.

percentile (green). We consider the frequencies that are most correlated with Brix and Dry Matter readings; therefore, we set a variable threshold (e.g., 0.25) and select the frequency bands for which the median normalized PLSR coefficients exceed that threshold. These selected bands are depicted as red regions in each plot of Fig. 11. Once these bands are identified, AgriTera can utilize the variation within these bands to predict ripeness metrics.

We make the following observations: first, the PLSR coefficients exhibit a similar pattern for green apples, whether they are being used to estimate Brix or Dry Matter. Once again, this demonstrates that Brix and Dry Matter are correlated. Second, the contribution of different frequencies varies depending on the fruit type. This shows that each fruit has its own distinct characteristics, and the same coefficient matrices cannot be applied universally to all fruits. Finally, the relatively small

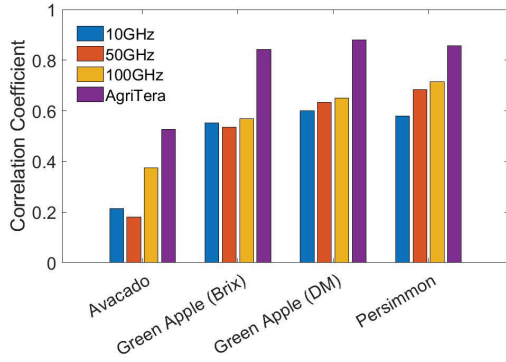


**Figure 12: Impact of Bandwidth on Performance.** The figure plots the correlation coefficient between the predicted ripeness metrics and the measured values for different sub-THz bandwidths and fruit types. We observe that increasing the bandwidth generally increases the correlation coefficient.

variation between the 25<sup>th</sup> and the 75<sup>th</sup> percentile indicates that a similar set of frequencies exhibit high sensitivity to chemical interactions that happen over time across different samples of the same fruit, despite potential differences in their exact size and geometry and orientation.

Second, Fig. 11 reveals that a wide range of frequencies have high sensitivity to changes in Brix and Dry Matter. This observation suggests that a wideband wireless transmission is needed to accurately estimate fruit ripening. To investigate this, we assess the performance of our model under a narrowband analysis. To have a fair comparison among different fruit types, we select a center frequency of 170 GHz as it shows high sensitivity to Brix and Dry matter among all fruits. We consider different bandwidths of 10, 50, and 100 GHz around this center frequency to evaluate the prediction accuracy as a function of bandwidth.

Fig. 12 displays the correlation coefficient, which indicates how closely the predicted values match the actual measured values. A higher correlation coefficient means that there is a stronger relationship between the predicted and measured values, implying a more accurate estimation. The purple bar in Fig. 12 represents the performance of AgriTera when it combines the spectral information from all of the shaded bands in Fig. 11. We observe that the prediction generally improves with larger bandwidth as a richer spectral signature can be used for estimation. The performance gap is not uniform, e.g., a larger gap in green apples and a lower gap in persimmon prediction.

These findings suggest that leveraging mmWave or WiFi for high-resolution fruit-quality sensing is not straightforward due to their limited bandwidth. Specifically, Green Apple and Persimmon have strong signatures around 0.4 THz which lies

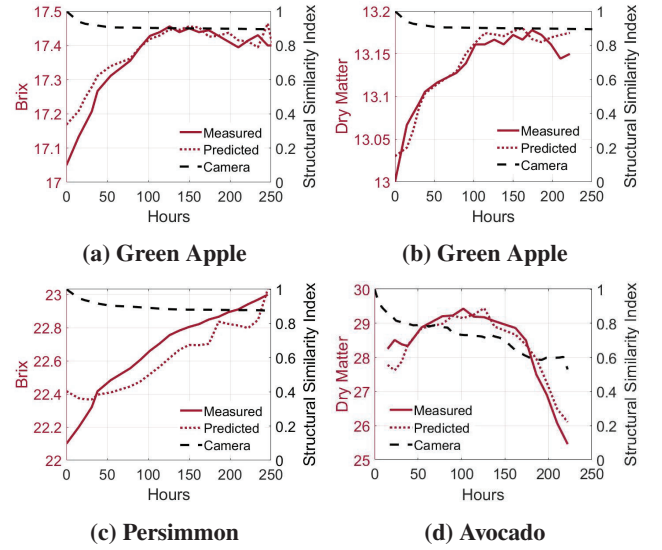


**Figure 13: AgriTera ripeness prediction during the ripening cycle.** The performance of AgriTera is compared against ground truth and our camera-based baseline scheme.

outside of the WiFi and mmWave bands. Moreover, relying on multiple narrowband systems is not feasible because the band of interest is fruit specific. Indeed, wideband sub-THz transmission is a great candidate for the ripeness sensing application.

#### 5.4 Ripeness Estimation Performance

Here, we assess the performance of AgriTera for different types of fruits. To this end, we generate predicted values for each fruit category over time and plot the median of these values for all samples of the same fruit type. Fig. 13 plots the predicted values and the measured values for Brix and Dry Matter for all three fruit types as a function of time. The root means square cross-validation (RMSECV) errors are 0.38, 0.13, 0.04, and 0.015 for avocado, persimmon, green apple (brix), and green apple (dry matter), respectively. These correspond to normalized RMSE (NRMSE) of 1.3%, 0.56%, 0.23%, and 0.1% (NRMSE is the RMSE error as a percentage of the mean of measured values). These percentages are within acceptable levels if they are well below 10% as they do not impact taste [26] and hence imperceivable by the consumers.

We compare the changes in Brix and Dry Matter to variations in images captured by cameras. In particular, we take pictures of the fruits with a high-resolution RGB camera every 12 hours and plot the structural similarity values (SSIM) over time to detect changes in the color of the fruit. Compared to other known metrics, such as peak signal-to-noise ratio or mean square error, SSIM is more in line with human visual perception and can better reflect the changes in the parameters



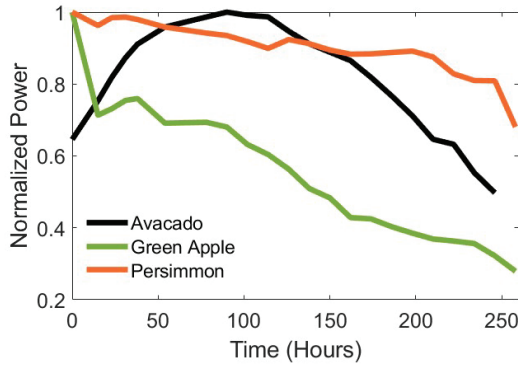


**Figure 14: Reflectance vs. Time.** This figure plots the power of the reflected sub-THz signal (in the band of 50 - 600 GHz) as a function of time when the fruit transitions from unripe to ripe, and post-ripe.

of the fruit images[23]. We used the first image as a reference and then calculated the changes in the subsequent images by computing the SSIM values. The SSIM values range from 0 to 1, where a low value indicates noticeable changes in the images and a value close to 1 indicates negligible changes. In Fig. 13, the SSIM values for various fruits are shown and compared against AgriTera’s performance. It is evident that the SSIM values generally decrease from 1 to 0.9 over the course of 10 days, but the change happens slowly and lacks the necessary detail to accurately predict different stages of ripeness (avocados are the exception but the SSIM value decline occur in the overripe stages). Therefore, such vision-based inferences are not an ideal choice to assess fruit quality as they rely solely on surface-level image data. In contrast, AgriTera can successfully map spectral signatures to Brix and Dry Matter estimates. The wider range of Brix/Dry matter values in the training data for persimmon and avocado results in higher prediction errors due to limited samples for each value. This can be resolved by expanding the training dataset to enhance accuracy.

### 5.5 Post-Ripe Inferences

Although past research has shown that Brix and Dry Matter are important metrics for determining horticulture maturity in fruits, they often do not indicate any information about the post-ripe stage. This is because they rely on the nutrient content in the fruit, which stops changing after horticulture maturity is reached (with the exception of avocados, which undergo nutrient decomposition during rotting). As we previously saw in Fig. 10, the Brix and Dry Matter values for Green Apple and Persimmon reach a plateau when the fruit is ripe. Hence, these readings do not provide a robust way to infer the quality of the fruit (is it edible or rotten). In contrast, we see a different trend with AgriTera. Fig. 14 shows the normalized reflected power from various fruits over time, computed using a frequency

band from 50 GHz to 600 GHz. As shown, the power values for both apple and persimmon continue to decay over time. This phenomenon occurs primarily because, over time, the fruits lose moisture, causing them to become more transparent to the sub-THz signal. Consequently, the reflected power decreases. This result is also in agreement with the findings in the initial feasibility experiment discussed in Section §5.1. Fig. 14 also shows the trend for avocados which is slightly different than persimmons and green apples: initially, the reflected power from avocados increases, primarily due to the accumulation of fatty acids in the mesocarp. However, over time, the power decreases due to the breakdown of the cell wall, causing the avocado skin to soften, and the moisture from the fruit to escape [13, 52]. This observation suggests that AgriTera can provide inferences about fruit quality in the over-ripe stage as well, unlike commercial specialized sensors. For instance, even if the Brix and Dry Matter values for certain fruits plateau over time, we can still utilize the decaying values of the reflected sub-THz energy to assess the state of the fruit beyond its ripe stage. This capability is indeed important to identify when a fruit is about to rot, allowing early intervention and preventing fruit waste. However, we need new metrics that can characterize the stage of rotting (over-maturing) and we will investigate this in future works.

## 6 RELATED WORK

The development of technologies for fruit monitoring and ripeness sensing has been the focus of a large number of research studies. Specifically, previous research has been conducted on measuring the refractive index of fruits and vegetables using specialized setups and THz spectroscopy [8]. These efforts consider a thin sample of the fruit in a controlled setup where the RX captures the signal that travels through the sample. Hence, to make sure that the signal is not blocked by the fruit, it is necessary to extract a thin slice (a few microns) of the fruit sample in these techniques [22]. While these efforts can provide an accurate measurement of the refractive index of the fruit sample, they are not suitable in practice. Indeed, cutting the fruit is destructive, and would change the ripening cycle. Other efforts include THz spectroscopy for foreign body detection (hair, insects, etc) and nutrient content analysis using permittivity and refractive index or detecting ethylene gas which contributes substantially to ripening [28, 57]. However, these schemes require calibrated setups which often include vacuumed chambers.

Previous research has also explored the use of wireless signals for Brix or moisture content estimation. However, these approaches have certain limitations. For instance, [61] estimates Brix by putting TX and RX in direct contact with the fruit body and at several positions to combat the inherent fruit transmission loss. However, this approach requires extensive

labor and does not provide the Dry Matter estimates needed for non-sugary fruits (e.g., avocados). Further, in [35], the authors exploit CSI measurements at WiFi frequencies and fuse them with vision. However, this approach requires exact phase measurements (calibrated with and without the fruit) which hinders its performance in multipath settings, dynamic environments, and when multiple fruits are within the range. Further, the accuracy is inherently lower due to the use of WiFi frequencies. Additionally, the authors in [49] employ machine learning models like SVM on THz measurements, but their approach requires slicing the fruit and can only provide discrete qualitative values (e.g., "fresh," "stale," etc.). In contrast, AgriTera offers accurate Brix and Dry Matter detection on a continuous scale, without direct contact, phase extraction, and destroying the fruit.

Since prior techniques require a lot of calibration, time, and effort to extract fruit quality metrics, recent proposals employ computer-vision algorithms to determine defects or color changes from fruit images[5, 34, 39]. Others looked at hyper-spectral imaging for identifying freshness and degree of maturity[53], however, cameras that can perform hyper-spectral imaging are still limited to extracting information from the peel of the fruit which is not very sensitive for various fruit types, while AgriTera can also infer about fruit quality by obtaining data from beneath the peel.

In contrast to these prior efforts, our system focuses on scalable, non-invasive, and wireless fruit ripeness sensing. More specifically, we make use of the dependence between the reflection properties of different fruits and their ripeness.

## 7 DISCUSSION & FUTURE WORK

**Impact of peel texture.** AgriTera relies on reflection off of the fruit body (and its internal pulp) for ripeness sensing. Hence, for fruits with non-smooth peels (e.g., avocados, kiwis, pineapples, etc), the amount of reflected power back to the RX can be significantly lower, yielding potentially higher estimation errors. Another challenge is that the surface texture would itself leave a spectral footprint on the sub-THz spectra [55]. Indeed, distinguishing the contribution of surface texture from the ripeness-related profile is an open problem. In the future, we will investigate the impact of the texture of the peel on ripeness inference.

**Mobile applications.** Given the lack of any widely available and cost-efficient food sensing device, consumers are often left to judge fruit quality based on its appearance. Hence, bringing this technology to future smartphones can be a game changer, allowing consumers to choose based on their diet and taste preferences leading to better eating habits and healthy diets. Enabling a mobile system for fruit sensing can also empower farmers to efficiently monitor the ripeness stage of fruits, allowing them to harvest at the optimal time. The main

challenge is to have sub-THz transceivers that can work with the power constraints of handheld devices [31, 46].

The potential of sub-THz bands in realizing ultra-fast connectivity and high-resolution localization [17–19, 32] has made it a promising candidate for next-generation networks, hence, it is expected that future mobile devices will have high-frequency transmission/reception capabilities. Broadband transceivers have already been implemented at low-cost and scalable CMOS technologies [10, 51, 54]. However, mobile fruit sensing has various practical challenges. Namely, changes in the position, distance, and orientation of fruit relative to the mobile device would cause fluctuations in the reflected received signal. Hence, we will investigate the challenges of extending AgriTera to future mobile applications.

**Other sensing use cases.** While this paper mainly focuses on fruit ripeness sensing, in principle, similar techniques be used to estimate other quality metrics, such as nutrient content. Additionally, it can also be utilized in safety standards to detect foreign bodies in the food, such as dead insects. This is possible because sub-THz signals can penetrate the food surface and provide information about what is happening beneath the surface, without the need for direct contact with the food item. Another use case for this technology could be to determine wine quality by monitoring the fermentation process and measuring the changes in sugar content over time. Yet, these use cases require separate modeling and we leave them for future work.

## 8 CONCLUSION

AgriTera marks an important step towards non-destructive, contact-free, and scalable fruit quality sensing using sub-THz bands. Our evaluation demonstrated that AgriTera is able to infer fruit quality metrics for different fruit types with high accuracy regardless of their shape, structure, or orientation. As the research evolves, we hope that it can continue to make non-invasive and wireless fruit and produce sensing technology more accessible to the general public, enabling them to have greater access to food and product safety solutions.

## 9 ACKNOWLEDGEMENTS

We appreciate the valuable comments and feedback from the anonymous reviewers. This research was supported by NSF grant number CNS-2313233 and Microsoft Research. We also thank Andrew He for his contribution to developing the camera setup in our experiments.

## REFERENCES

- [1] 2014. Food Loss—Questions About the Amount and Causes Still Remain. <https://www.ers.usda.gov/amber-waves/2014/june/food-loss-questions-about-the-amount-and-causes-still-remain/> Accessed: 2023-03-11.
- [2] 2022. Food Waste Research. <https://www.epa.gov/land-research/food-waste-research#why> Accessed: 2023-03-11.
- [3] 2023. Food Waste and Food Resue. <https://www.feedingamerica.org/our-work/reduce-food-waste> Accessed: 2023-03-11.
- [4] 2023. How Many Fruits and Veggies do We Waste per Year? <https://www.goruvi.com/blogs/news/644-million-tons-of-wasted-fruits-and-veggies-each-year> Accessed: 2023-03-11.
- [5] Israel Arzate-Vázquez, José Jorge Chanona-Pérez, María de Jesús Perea-Flores, Georgina Calderón-Domínguez, Marco A Moreno-Armendáriz, Hiram Calvo, Salvador Godoy-Calderón, Roberto Quevedo, and Gustavo Gutiérrez-López. 2011. Image Processing Applied to Classification of Avocado Variety Hass (*Persea americana* Mill.) during the Ripening Process. *Food and Bioprocess Technology* 4 (2011), 1307–1313.
- [6] Richard D Averitt, Willie J Padilla, Hou-Tong Chen, John F O'Hara, Antoinette J Taylor, Clark Highstrete, Mark Lee, Joshua M.O. Zide, SR Bank, and Arthur C Gossard. 2007. Terahertz Metamaterial Devices. In *Terahertz Physics, Devices, and Systems II*, Vol. 6772. SPIE, 23–31.
- [7] Cornelius Barry and James Giovannoni. 1997. Ethylene and Fruit Ripening. *Journal of Plant Growth Regulation* 26 (01 1997).
- [8] Maxime Bernier, Frédéric Garet, and Jean-Louis Coutaz. 2017. Determining the Complex Refractive Index of Materials in the Far-Infrared from Terahertz Time-Domain Data. In *Terahertz Spectroscopy*, Jamal Uddin (Ed.). IntechOpen, Rijeka, Chapter 7.
- [9] Indu Chandrasekaran, Shubham Panigrahi, Lankapalli Ravikanth, and Chandra Singh. 2019. Potential of Near-Infrared (NIR) Spectroscopy and Hyperspectral Imaging for Quality and Safety Assessment of Fruits: an Overview. *Food Analytical Methods* 12 (11 2019).
- [10] Taiyun Chi, Min-Yu Huang, Sensen Li, and Hua Wang. 2017. 17.7 A Packaged 90-to-300GHz Transmitter and 115-to-325GHz Coherent Receiver in CMOS for Full-Band Continuous-wave mm-Wave Hyperspectral Imaging. In *Proc. of IEEE ISSCC*.
- [11] Kim Seng Chia, Mohamad Nur Hakim Jam, Zeanne Gan, and Nurlaila Ismail. 2020. Pre-dispersive Near-infrared Light Sensing in Non-destructively Classifying the Brix of Intact Pineapples. *Journal of Food Science and Technology* 57 (2020), 4533–4540.
- [12] Bryan G. Coombe, Robert J. Dundon, and Andrew W. S. Short. 1980. Indices of Sugar—acidity as Ripeness Criteria for Winegrapes. *Journal of the Science of Food and Agriculture* 31, 5 (1980), 495–502.
- [13] Bruno G Defilippi, Troy Ejsmentewicz, María Paz Covarrubias, Orianne Gudenschwager, and Reinaldo Campos-Vargas. 2018. Changes in cell wall pectins and their relation to postharvest mesocarp softening of “Hass” avocados (*Persea americana* Mill.). *Plant Physiology and Biochemistry* 128 (2018), 142–151.
- [14] Manoj Dora, Joshua Wesana, Xavier Gellynck, Nitin Seth, Bidit Dey, and Hans De Steur. 2020. Importance of Sustainable Operations in Food Loss: Evidence from the Belgian Food Processing Industry. *Annals of operations research* 290 (2020), 47–72.
- [15] Birgit Esser, Jan M Schnorr, and Timothy M Swager. 2012. Selective detection of ethylene gas using carbon nanotube-based devices: utility in determination of fruit ripeness. *Angewandte Chemie International Edition* 51, 23 (2012), 5752–5756.
- [16] Felix. [n. d.]. F-750 Produce Quality Meter. <https://felixinstruments.com/>
- [17] Yasaman Ghasempour, Yasith Amarasinghe, Chia-Yi Yeh, Edward Knightly, and Daniel M Mittleman. 2021. Line-of-sight and non-line-of-sight links for dispersive terahertz wireless networks. *APL Photonics* 6, 4 (2021).
- [18] Yasaman Ghasempour, Rabi Shrestha, Aaron Charous, Edward Knightly, and Daniel M Mittleman. 2020. Single-shot link discovery for terahertz wireless networks. *Nature communications* 11, 1 (2020), 2017.
- [19] Yasaman Ghasempour, Chia-Yi Yeh, Rabi Shrestha, Yasith Amarasinghe, Daniel Mittleman, and Edward W Knightly. 2020. LeakyTrack: Non-coherent single-antenna nodal and environmental mobility tracking with a leaky-wave antenna. In *SenSys' 20: Proceedings of the 18th Conference on Embedded Networked Sensor Systems*.
- [20] Gregory Gougeon, Yoann Corre, and Mohammed Zahid Aslam. 2019. Ray-based Deterministic Channel Modelling for sub-THz Band. In *2019 IEEE 30th International Symposium on Personal, Indoor and Mobile Radio Communications (PIMRC Workshops)*. 1–6.
- [21] Aoife Gowen, Cr  idhe O'Sullivan, and Colm O'Donnell. 2012. Terahertz Time Domain Spectroscopy and Imaging: Emerging Techniques for Food Process Monitoring and Quality Control. *Trends in Food Science & Technology* 25, 1 (2012), 40–46.
- [22] Aoife Gowen, Cr  idhe O'Sullivan, and Colm O'Donnell. 2012. Terahertz time domain spectroscopy and imaging: Emerging Techniques for Food Process Monitoring and Quality Control. *Trends in Food Science & Technology* 25, 1 (2012), 40–46.
- [23] Mohammed Hassan and Chakravarthy Bhagvati. 2012. Structural Similarity Measure for Color Images. *International Journal of Computer Applications* 43, 14 (2012), 7–12.
- [24] Wen-Ding Huang, Sanchali Deb, Young-Sik Seo, Smitha Rao, Mu Chiao, and J. C. Chiao. 2012. A Passive Radio-Frequency pH-Sensing Tag for Wireless Food-Quality Monitoring. *IEEE Sensors Journal* 12, 3 (2012), 487–495.
- [25] Rovshen Ishangulyev, Sanghyo Kim, and Sang Hyeon Lee. 2019. Understanding Food Loss and Waste — Why are We Losing and Wasting Food? *Foods* 8, 8 (2019), 297.
- [26] Peter D Jamieson, John R Porter, and DR Wilson. 1991. A Test of the Computer Simulation Model ARCWHEAT1 on Wheat Crops Grown in New Zealand. *Field crops research* 27, 4 (1991), 337–350.
- [27] Steffen Janssen, Katrin Schmitt, Michael Blanke, Marie-Luise Bauersfeld, J  rgen W  llenstein, and Walter Lang. 2014. Ethylene Detection in Fruit Supply Chains. *Philosophical Transactions of the Royal Society A: Mathematical, Physical and Engineering Sciences* 372, 2017 (2014), 20130311.
- [28] Christian J  rdens, Maik Scheller, Bj  rn Breitenstein, Dirk Selmar, and Martin Koch. 2009. Evaluation of Leaf Water Status by Means of Permittivity at Terahertz Frequencies. *Journal of biological physics* 35 (2009), 255–264.
- [29] Toru Katsumata, Hiroaki Aizawa, Shuji Komuro, Shigeo Ito, and Takeshi Matsumoto. 2019. Non-destructive Evaluation of Orange Juice Based on Optical Scattering Intensities. *Optik* 182 (2019), 1064–1073.
- [30] Matthew D. Kleinhenz and Natalie R. Bumgarner. 2013. Using  $\circ$  Brix as an Indicator of Vegetable Quality An Overview of the Practice.
- [31] Atsutse Kludze and Yasaman Ghasempour. 2023. {LeakyScatter}: A {Frequency-Agile} Directional Backscatter Network Above 100 {GHz}. In *20th USENIX Symposium on Networked Systems Design and Implementation (NSDI 23)*. 375–388.
- [32] Atsutse Kludze, Rabi Shrestha, Chowdhury Miftah, Edward Knightly, Daniel Mittleman, and Yasaman Ghasempour. 2022. Quasi-optical 3D localization using asymmetric signatures above 100 GHz. In *Proceedings of the 28th Annual International Conference on Mobile Computing And Networking*. 120–132.
- [33] Erika Kress-Rogers and Christopher JB Brimelow. 2001. *Instrumentation and Sensors for the Food Industry*. Vol. 65. Woodhead Publishing.
- [34] Shreya Lal, Santi Kumari Behera, Prabira Kumar Sethy, and Amiya Kumar Rath. 2017. Identification and Counting of Mature Apple Fruit Based on BP Feed Forward Neural Network. In *2017 Third International Conference on Sensing, Signal Processing and Security (ICSSS)*. IEEE,



- 361–368.
- [35] Yutong Liu, Landu Jiang, Linghe Kong, Qiao Xiang, Xue Liu, and Guihai Chen. 2022. Wi-Fruit: See Through Fruits with Smart Devices. 5, 4 (2022).
- [36] Luna. 2018. The TeraMetrix T-Ray® 5000 Series Intelligent Terahertz Control Unit. <https://lunainc.com/blog/terametrix-t-rayr-5000-series-intelligent-terahertz-control-unit>
- [37] W. B. McGlasson. 1985. Ethylene and Fruit Ripening. *HortScience* 20, 1 (1985), 51–54.
- [38] Daniel M. Mittleman, Rune H. Jacobsen, and Martin C. Nuss. 1996. T-ray Imaging. *IEEE Journal of Selected Topics in Quantum Electronics* 2, 3 (1996), 679–692.
- [39] Vahid Mohammadi, Kamran Kheiralipour, and Mahdi Ghasemi-Varnamkhasti. 2015. Detecting Maturity of Persimmon Fruit Based on Image Processing Technique. *Scientia Horticulturae* 184 (2015), 123–128.
- [40] Siddhanth (Sid) Mookerjee, Yann Cornil, and JoAndrea Hoegg. 2021. From Waste to Taste: How “Ugly” Labels Can Increase Purchase of Unattractive Produce. *Journal of Marketing* 85, 3 (2021), 62–77.
- [41] Leandro Oliveira and Adriana Franca. 2011. Applications of Near Infrared Spectroscopy (NIRS) in Food Quality Evaluation. *Food Quality: Control, Analysis and Consumer Concerns* (02 2011), 131–180.
- [42] Daniel I. Onwude, Guangnan Chen, Nnanna Eke-emezie, Abraham Kabutey, Alfadhl Yahya Khaled, and Barbara Sturm. 2020. Recent Advances in Reducing Food Losses in the Supply Chain of Fresh Agricultural Produce. *Processes* 8, 11 (2020).
- [43] John Palmer, F. Harker, D Tustin, and Jason Johnston. 2010. Fruit Dry Matter Concentration: A New Quality Metric for Apples. *Journal of the science of food and agriculture* 90 (12 2010), 2586–94.
- [44] Vijay Paul, Rakesh Pandey, and Girish C Srivastava. 2012. The Fading Distinctions between Classical Patterns of Ripening in Climacteric and Non-climacteric Fruit and the Ubiquity of Ethylene — An Overview. *Journal of food science and technology* 49 (2012), 1–21.
- [45] Sastia Prama Putri, Muhammad Maulana Malikul Ikram, Arisa Sato, Hadi Akbar Dahlan, Della Rahmawati, Yukina Ohto, and Ei-ichiro Fukusaki. 2022. Application of Gas Chromatography-mass Spectrometry-based Metabolomics in Food Science and Technology. *Journal of Bioscience and Bioengineering* (2022).
- [46] Hamed Rahmani, Darshan Shetty, Mahmoud Wagih, Yasaman Ghasempour, Valentina Palazzi, Nuno B Carvalho, Ricardo Correia, Alessandra Costanzo, Dieff Vital, Federico Alimenti, et al. 2023. Next-generation IoT devices: Sustainable eco-friendly manufacturing, energy harvesting, and wireless connectivity. *IEEE Journal of Microwaves* 3, 1 (2023), 237–255.
- [47] Robin Raju, Greg E. Bridges, and Sharmistha Bhadra. 2020. Wireless Passive Sensors for Food Quality Monitoring: Improving the Safety of Food Products. *IEEE Antennas and Propagation Magazine* 62, 5 (2020), 76–89.
- [48] Aifeng Ren, Adnan Zahid, Xiaodong Yang, Akram Alomainy, Muhammad Imran, and Qammer Abbasi. 2019. Terahertz (THz) Application in Food Contamination Detection. (12 2019).
- [49] Aifeng Ren, Adnan Zahid, Ahmed Zoha, Syed Aziz Shah, Muhammad Ali Imran, Akram Alomainy, and Qammer H Abbasi. 2019. Machine learning driven approach towards the quality assessment of fresh fruits using non-invasive sensing. *IEEE Sensors Journal* 20, 4 (2019), 2075–2083.
- [50] Yili Ren, Sheng Tan, Linghan Zhang, Zi Wang, Zhi Wang, and Jie Yang. 2020. Liquid Level Sensing Using Commodity WiFi in a Smart Home Environment. *Proc. ACM Interact. Mob. Wearable Ubiquitous Technol.* 4, 1, Article 24 (mar 2020), 30 pages.
- [51] Patrick Reynaert, Wouter Steyaert, Alexander Standaert, Dragan Simic, and Guo Kaizhe. 2017. mm-Wave and THz Circuit Design in Standard CMOS Technologies: Challenges and Opportunities. In *2017 IEEE Asia Pacific Microwave Conference (APMC)*. IEEE, 85–88.
- [52] Carlos Eduardo Rodríguez-López, Carmen Hernández-Brenes, Víctor Treviño, and Rocío I Díaz de la Garza. 2017. Avocado Fruit Maturation and Ripening: Dynamics of Aliphatic Acetogenins and Lipidomic Profiles from Mesocarp, Idioblasts and Seed. *BMC plant biology* 17, 1 (2017), 1–23.
- [53] James Rogers. 2021. See Beyond the Peel. <https://www.a Peel.com/blog/see-beyond-the-peel>
- [54] Kaushik Sengupta and Ali Hajimiri. 2012. A 0.28 THz Power-Generation and Beam-Steering Array in CMOS based on Distributed Active Radiators. *IEEE Journal of Solid-State Circuits* 47, 12 (2012), 3013–3031.
- [55] Ruiyi Shen and Yasaman Ghasempour. 2023. Rough Surfaces Scattering and Mobility-Resilient Terahertz Wireless Links. In *2023 48th International Conference on Infrared, Millimeter and Terahertz Waves (IRMMW-THz)*. 1–2.
- [56] KP Sudheer and V Indira. 2007. *Post Harvest Technology of Horticultural Crops*. Vol. 7. New India Publishing.
- [57] Xudong Sun, Jiajun Li, Yun Shen, and Wenping Li. 2021. Non-destructive Detection of Insect Foreign Bodies in Finishing Tea Product Based on Terahertz Spectrum and Image. *Frontiers in Nutrition* 8 (2021), 757491.
- [58] Ee Lim Tan, Wen Ni Ng, Ranyuan Shao, Brandon D Pereles, and Keat Ghee Ong. 2007. A Wireless, Passive Sensor for Quantifying Packaged Food Quality. *Sensors* 7, 9 (2007), 1747–1756.
- [59] Sheng Tan, Linghan Zhang, and Jie Yang. 2018. Sensing Fruit Ripeness Using Wireless Signals. In *2018 27th International Conference on Computer Communication and Networks (ICCCN)*. 1–9.
- [60] Rucha Thakur, Gaurav Suryawanshi, Hardik Patel, and Janhavi Sangoi. 2020. An Innovative Approach For Fruit Ripeness Classification. In *2020 4th International Conference on Intelligent Computing and Control Systems (ICICCS)*. 550–554.
- [61] Zhicheng Yang, Parth H Pathak, Mo Sha, Tingting Zhu, Junai Gan, Pengfei Hu, and Prasant Mohapatra. 2019. On the Feasibility of Estimating Soluble Sugar Content using Millimeter-wave. In *Proceedings of the International Conference on Internet of Things Design and Implementation*. 13–24.
- [62] Borwen You, Ching-Yu Chen, Chin-Ping Yu, Pei-Hwa Wang, and Ja-Yu Lu. 2018. Frequency-Dependent Skin Penetration Depth of Terahertz Radiation Determined by Water Sorption-desorption. *Opt. Express* 26, 18 (Sep 2018), 22709–22721.
- [63] Guozhong Zhao, Maarten Ter Mors, Tom Wenckebach, and Paul CM Planken. 2002. Terahertz Dielectric Properties of Polystyrene Foam. *JOSA B* 19, 6 (2002), 1476–1479.